The Santa Cruz Eddy. Part II: Mechanisms of Formation

CRISTINA L. ARCHER AND MARK Z. JACOBSON

Stanford University, Stanford, California

(Manuscript received 25 March 2004, in final form 1 February 2005)

ABSTRACT

The formation mechanism of the Santa Cruz eddy (SCE) is investigated using the fifth-generation Pennsylvania State University–National Center for Atmospheric Research Mesoscale Model (MM5). Simulations of 25–26 August 2000 showed that two eddy instances formed on that night, a finding supported by observations. The two eddies had similar behavior: they both formed in the sheltered Santa Cruz, California, area and then moved southeastward, to finally dissipate after 7–11 h. However, the first eddy had greater vorticity, wind speed, horizontal and vertical extents, and lifetime than the second eddy. Numerical simulations showed that the SCEs are formed by the interaction of the main northwesterly flow with the topographic barrier represented by the Santa Cruz Mountains to the north of Monterey Bay. Additional numerical experiments were undertaken with no diurnal heating cycle, no (molecular or eddy) viscosity, and no horizontal thermal gradients at ground level. In all cases, vertical vorticity was still created by the tilting of horizontal vorticity generated by the solenoidal term in the vorticity equation. This baroclinic process appeared to be the fundamental formation mechanism for both SCEs, but more favorable conditions in the late afternoon (including a south-to-north pressure gradient, flow turning due to the sea breeze, and an expansion fan) coincided to intensify the first eddy.

1. Introduction

In Archer and Jacobson (2005), a cyclonic vortex that forms in the summer over Monterey Bay (California), the Santa Cruz eddy (SCE), was investigated from the observational point of view. A limited mesonet of 10 surface stations was able to provide information about several aspects of the eddy (such as timing and correlation with pressure patterns) but was inadequate for finding the mechanism(s) of SCE formation. In this paper, each possible formation mechanism claimed for other known vortices is isolated and investigated via a numerical approach. First, results obtained for a test case will be presented in detail, with special emphasis on vorticity patterns. Then, a series of numerical tests will be introduced to evaluate the relative importance of individual factors, such as topography or viscosity, on eddy formation.

Corresponding author address: Cristina L. Archer, Department of Civil and Environmental Engineering, Stanford University, Stanford, CA 94305.
E-mail: lozej@stanford.edu

2. SCE simulations

The SCE event of 25–26 August 2000, described in Archer and Jacobson (2005), was chosen as the test case for the simulations. The model used in this study is the fifth-generation Pennsylvania State University–National Center for Atmospheric Research Mesoscale Model (MM5), described in Dudhia (1993). Initial and boundary conditions were provided by the Eta model, with ~40 km horizontal resolution; one-way nesting was imposed between the parent domain ("domain 1," with horizontal resolution of 5 km, 150 × 120 grid points, 29 vertical levels, and 15-s time step), which covers the entire California area, and a nested grid ("domain 2," with horizontal resolution of 1 km, 150 × 120 grid points, 29 vertical levels, and 3-s time step), centered on the Monterey Bay area (Fig. 1). The following parameterizations were selected: Eta Mellor–Yamada scheme for turbulence (Mellor and Yamada 1982; Janjić 1990, 1994); no cumulus parameterization; simple-ice explicit scheme for resolved precipitation (Hsie et al. 1984); cloud-radiation scheme (Stephens 1978); Ohio State University (OSU)/Eta land surface model (Pan and Mahrt 1987; Chen et al. 1996, 1997); no

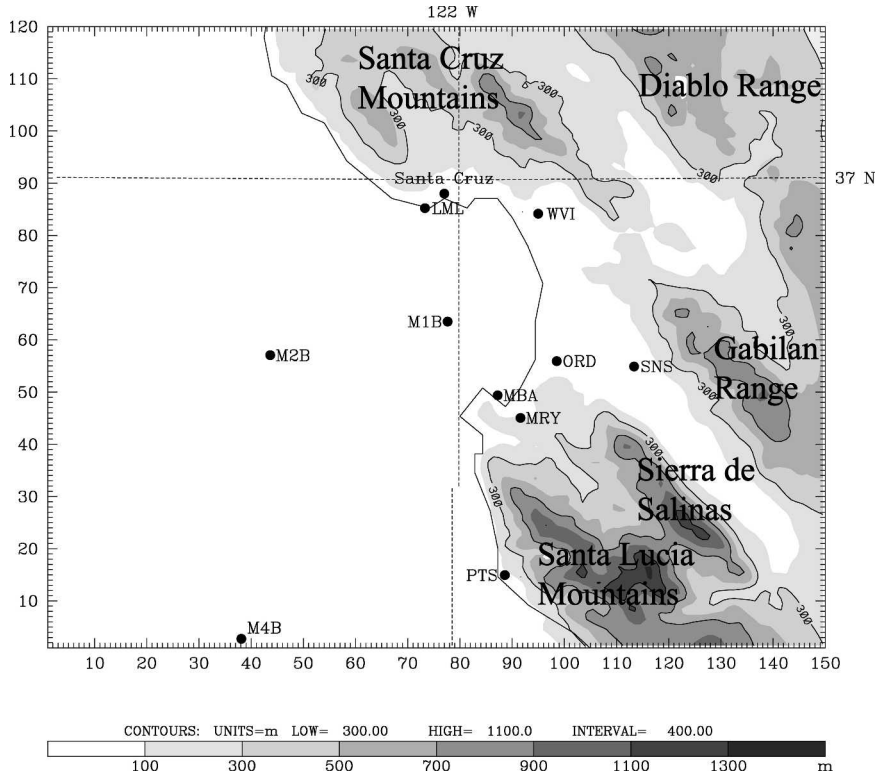

FIG. 1. Topography details of the Monterey Bay area (m, shaded) and station locations. The area shown coincides with the high-resolution domain (domain 2).

four-dimensional data assimilation. All runs started at 1200 UTC on 24 August 2000, a day before the day of interest, to allow the model to adjust to the initial conditions. The runs were carried out over 48–60 h.

In the next sections, the evolution of two SCE occurrences (indicated as first or evening eddy, and second or nocturnal eddy, respectively) simulated by MM5 will be presented at four times (unless otherwise stated): during the afternoon sea breeze (prior to the eddy formation), during the mature stage of the first SCE, during its dissipating phase, and during the mature stage of the second SCE.

a. Winds and vorticity

In the rest of this study, the Pacific daylight time (PDT) will be used, corresponding to −7 h from the coordinated universal time (UTC) in the summer. During the afternoon (1300 PDT), simulated 10-m wind streamlines (Fig. 2a) suggest that the flow over Monterey Bay was westerly (due to the sea breeze), whereas off the coast the main synoptic flow was northwesterly, parallel to the coast. Positive vorticity was formed along the coast, both to the north and to the south of the bay, due to horizontal shear caused by fast winds over water and slower winds over land (as roughness length varied from 0.01 cm over water to 50 cm over evergreen needle forest), friction against the sides of the Santa Cruz Mountains (SCM), and flow convergence due to the blocking effect of mountains. A detailed analysis of the vorticity formation will be introduced in section 3d.

The sea breeze was also responsible for the southerly flow to the east of Santa Cruz. Vorticity was created there as a result of two mechanisms: the turning of the flow from northwesterly at the entrance of the bay to southerly a few kilometers to the east, and advection of vorticity created along the coast to the northwest of Santa Cruz, as described above. Observed winds agree well with MM5 wind patterns in Fig. 2a, with the only exception being Watsonville (WVI), where the simulated flow was too westerly (see Fig. 1 for station locations).

Before and during the early stages of eddy formation, an area of high wind speed (greater than 6 $m\,s^{-1}$) formed offshore and to the west of Santa Cruz (Figs. 3a,b). According to Burk et al. (1999) and Burk and Haack (2000), an area of supercritical flow can form either at or past a convex bend in topography, such as the Monterey Bay. Supercritical conditions in atmospheric flow occur when the wind speed exceeds the

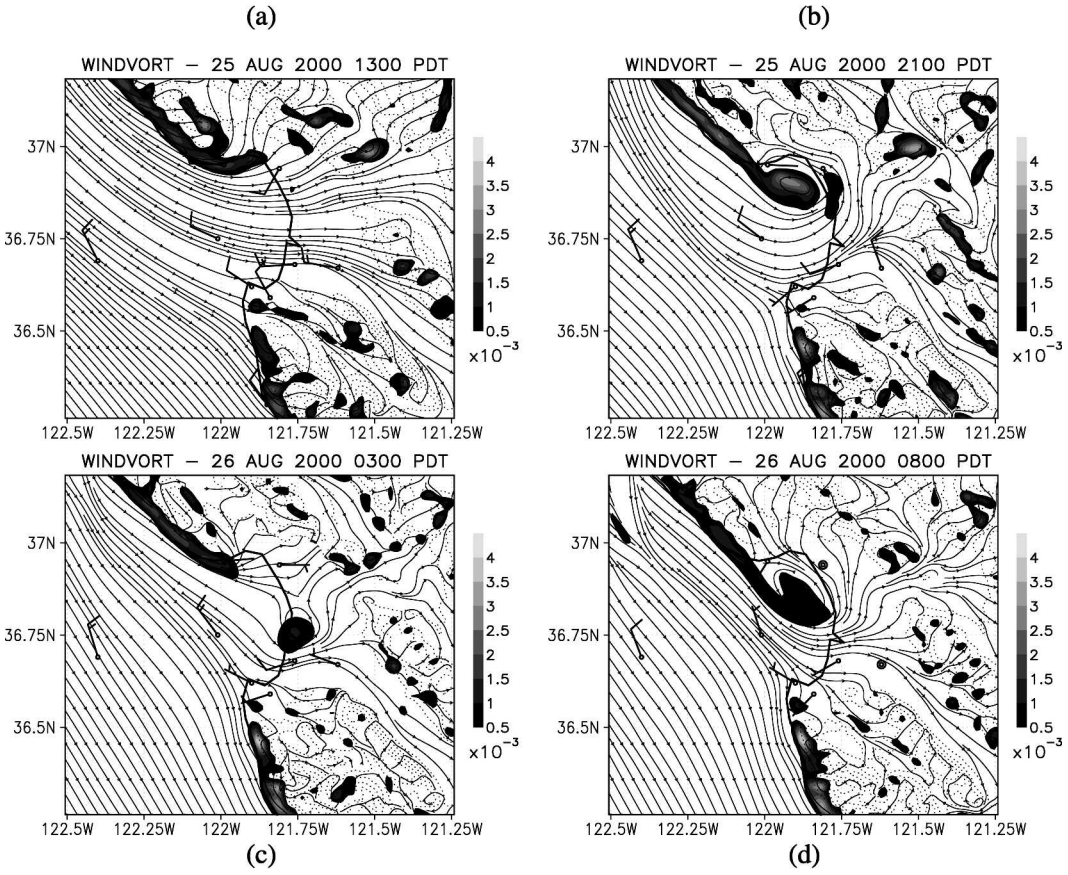

FIG. 2. Simulated streamlines of 10-m winds, observed wind barbs (1 barb = 1 kt = 0.94 m s^{-1}) at station locations, and simulated vertical vorticity (10^{-3} s^{-1}, gray shaded) on domain 2 during 25–26 Aug 2000 at key times of the SCE evolution: (a) sea breeze (1300 PDT); (b) mature stage of the first SCE occurrence (2100 PDT); (c) dissipating stage (0300 PDT); and (d) mature stage of the second SCE occurrence (0800 PDT). Terrain elevation is contoured with dotted lines every 200 m.

phase speed of internal gravity waves. If the area of supercritical flow forms past the convex bend and it is accompanied by divergence and by lowering of the boundary layer, then it is called an "expansion fan." If the flow does not reach supercritical conditions, the high (but not supercritical) speed area forms upstream from the bend (Burk et al. 1999). If U is the upstream wind speed, g' the reduced gravity $g \times (\Delta\theta/\theta)$ ($\Delta\theta$ is the difference in potential temperature θ across the inversion), and h the height of the marine boundary layer (MBL), the Froude number

$$\mathrm{Fr} = \frac{U}{\sqrt{g'h}} = \frac{U}{\sqrt{g\dfrac{\Delta\theta}{\theta}h}} \tag{1}$$

can be used to determine the flow criticality. Froude number values greater (smaller) than one indicate supercritical (subcritical) flow. However, this is strictly valid only under the shallow-water approximation and not when either stability or wind speed vary within a layer, as in the SCE case.

With these limitations in mind, approximate Fr values were calculated from the MM5 simulated flow following Haack et al. (2001). The value used for θ in Eq. (1) is the average potential temperature within the layer below the marine inversion, whose top is located at the height h where the potential temperature increase with height becomes less steep; U is the average wind speed in the layer, and $\Delta\theta$ is the difference between potential temperature at the inversion top and the average potential temperature below the inversion. For the flow upstream of Monterey Bay, Fr was approximately 0.66 (subcritical), whereas in the center of the accelerated flow Fr was ~1.12 (supercritical) during the day. These values were calculated at the subcritical point marked in Fig. 3a and at the supercritical point marked in Fig. 3c. The daytime average values were

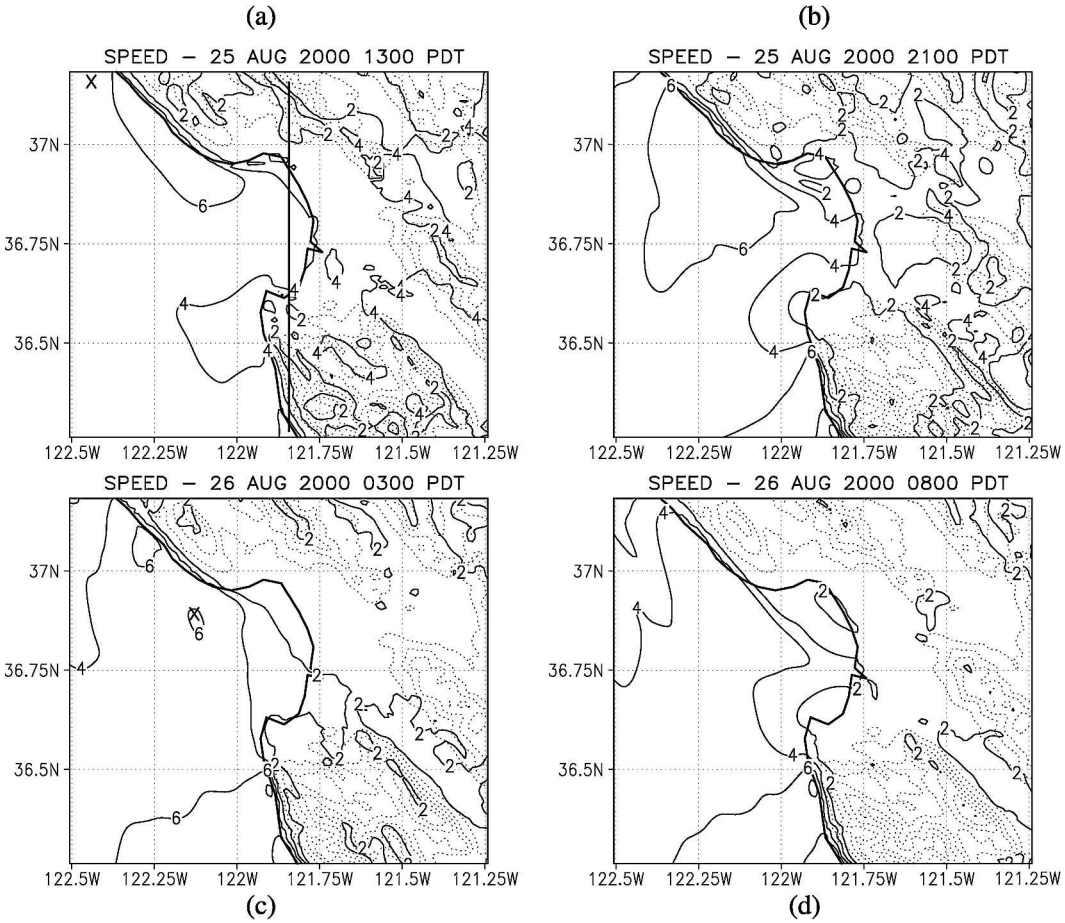

FIG. 3. Simulated wind speed (m s^{-1}, solid line every 2 m s^{-1}) on domain 2 during 25–26 Aug 2000 at key times of the SCE evolution: (a) sea breeze (1300 PDT); (b) mature stage of the first SCE occurrence (2100 PDT); (c) dissipating stage (0300 PDT); and (d) mature stage of the second SCE occurrence (0800 PDT). Terrain elevation is contoured with dotted lines every 200 m. The location of the north–south cross section discussed later is shown in (a). Cross marks indicate a subcritical point in (a) and a supercritical one in (c).

(with the subcritical value in parentheses) $\theta = 286$ (285) K; $\Delta\theta = 13$ (14) K; $U = 7.7$ (5.5) m s^{-1}; $h = 99$ (170) m; Fr = 1.12 (0.62). The 60-h averages were $\theta = 286$ (285) K; $\Delta\theta = 12$ (13) K; $U = 6.7$ (5.6) m s^{-1}; $h = 147$ (207) m; Fr = 0.96 (0.66). Given the location of the high wind speed area (i.e., past and not upstream of the bay), the approximate Fr greater than one, and the lowering of the MBL (not shown), the simulated high wind speed area can be considered an expansion fan. Expansion fans have been associated with scalloped areas of clearing from the fog in the lee of concave bendings along the California coast, including at the Monterey Bay entrance, by Haack et al. (2001) and Koračin and Dorman (2001).

Observations showed that the first SCE formed at about 1700 PDT, whereas model results showed the first appearance of a closed circulation only 2 h later, at 1900 PDT (not shown). Like the observed one, it was initially limited to the northeastern portion of the bay. The mature stage of the simulated eddy was reached at about 2100 PDT (Fig. 2b), where closed streamlines and high vorticity define the presence of the SCE. Model results are in good agreement with observations at all stations.

The SCE detached from the SCM and moved southeastward in the next hours. In the rest of the paper, the fact that the eddy detaches from the mountains will be indicated as "vortex shedding." Technically, vortex shedding refers to the detachment of couples of counterrotating vortices in the (unstable) wake of an obstacle. Even though no anticyclonic eddy forms on the lee of the SCM, this notation will be used for the SCE because it is nonstationary, it detaches from the SCM, and it has multiple occurrences. Vortex shedding will be discussed further in section 4. Vorticity decreased in the eddy center as soon as it detached from the land (not shown). By 0600 PDT, about 2 h after reaching

land, the first SCE had completely dissipated. Vorticity was still forming along the northern coastline, where it will continue to form throughout the entire simulation. The expansion fan had disappeared at this hour, as only two small areas of wind speed greater than 6 m s^{-1} were left offshore at 0300 PDT (Fig. 3c).

At 0300 PDT, observations showed the presence of a second SCE offshore from Santa Cruz (not shown), but the simulated eddy was again delayed by about 2 h and reached its mature stage at about 0800 PDT (Fig. 2d). This second SCE occurrence was characterized by generally slower wind speeds and lower vorticity than the earlier one. It detached at 0900 and dissipated by 1000 PDT, when its core vorticity fell below 0.5×10^{-3} s^{-1}.

b. Temperature and pressure

During the day, the Santa Cruz area was characterized by not only the highest temperatures, but also the lowest relative humidities in the entire Monterey Bay (Archer 2004). Vice versa, Monterey was cloudy and had a temperature of ~14°C, ~6°C cooler than Santa Cruz. Moisture from the south bay was advected northward during the eddy, in a "wrapping" fashion. The first eddy had a warm core, as air with warmer temperature was trapped in the center of the circulation, whereas the second eddy had a cooler core, as it was formed with cooler air advected into the bay from the northern coast. Aside from that, the temperature and moisture fields over Monterey Bay became uniform at night; hence the SCE had a "homogenizing" effect on the bay.

The simulated sea level pressure pattern was consistent with the presence of lower pressure in the Santa Cruz area and relatively high pressure in the southern bay, as suggested by the observational analysis in Archer and Jacobson (2005). Simulated sea level pressure is shown in Fig. 4. Note the ridge of higher pressure along the eastern part of the bay prior to the eddy formation. During the mature stage of the first SCE, a local "low" formed near the center of the eddy, as indicated by the almost closed contour of the 1015-hPa isobar offshore from Santa Cruz (Fig. 4b). At this time, a light south-to-north pressure gradient was still present over the bay. However, during the dissipating stage (Fig. 4c), the south-to-north pressure gradient was destroyed too, leaving uniform pressure of about 1015 hPa over the whole Monterey Bay. The second SCE formed, therefore, without any south-to-north pressure gradient.

Trends of simulated sea level pressure at two key locations are shown in Fig. 5, together with the south-to-north pressure gradient between MRY (Monterey) and LML (Santa Cruz). The strength of the pressure gradient of the first eddy was well reproduced by MM5. Note that the maximum of the simulated pressure gradient was reached about 2 h after that of the observed one, just as the simulated eddy started 2 h after the observed one. However, the simulated second eddy formed without any pressure gradient. The absence of the second maximum of the simulated pressure gradient confirms that the south-to-north pressure gradient was not necessary for SCE formation. Note that observational findings in Archer and Jacobson (2005) showed that such a pressure gradient was not sufficient either.

c. Vertical structure

The MM5 performance was verified by comparing its results for Fort Ord (Fig. 6) with the observed profiler data shown in Fig. 5 of Archer and Jacobson (2005). Simulated (virtual) temperature showed the typical profile of a marine location, with cooler temperatures close to the ground and warmer air above. The simulated (and observed) inversion was not elevated but ground based; its top (where maximum temperatures were found) was located at about 500 m, as observed. However, the inversion strength was underestimated, as the observed maximum temperature was ~27°C, whereas the simulated maximum was only ~23°C. Near the surface, low temperatures were observed in the afternoon and in the early morning hours, whereas MM5 results showed only a nighttime minimum. The deepening of the MBL on 26 August was well simulated by MM5. Winds below 300 m were generally well reproduced by the model, although they showed a stronger westerly component than observed. Above the inversion, observed winds were light and chaotic up to 1000 m, but simulated winds showed a more westerly component. No clear indication of an SCE presence could be detected from the simulated or observed winds at Fort Ord.

In summary, simulated temperatures were too warm near the surface and too cold in the inversion, and simulated winds had a stronger westerly component than observed winds. However, MM5 successfully reproduced general trends of the MBL evolution, inversion location, and wind patterns in the lowest levels, which are the most important parameters for the SCE.

To describe the vertical structure of the two SCE occurrences of 25 August 2000, a cross section was selected, indicated in Fig. 3a. It was oriented north–south and was intended to show the influence of the Santa Cruz Mountains on the eddy. In the afternoon (Fig. 7a), light and subsiding winds occurred from 300 to 1000 m, except at the mountain tops, where higher temperatures caused upslope flow. The marine layer below 300 m

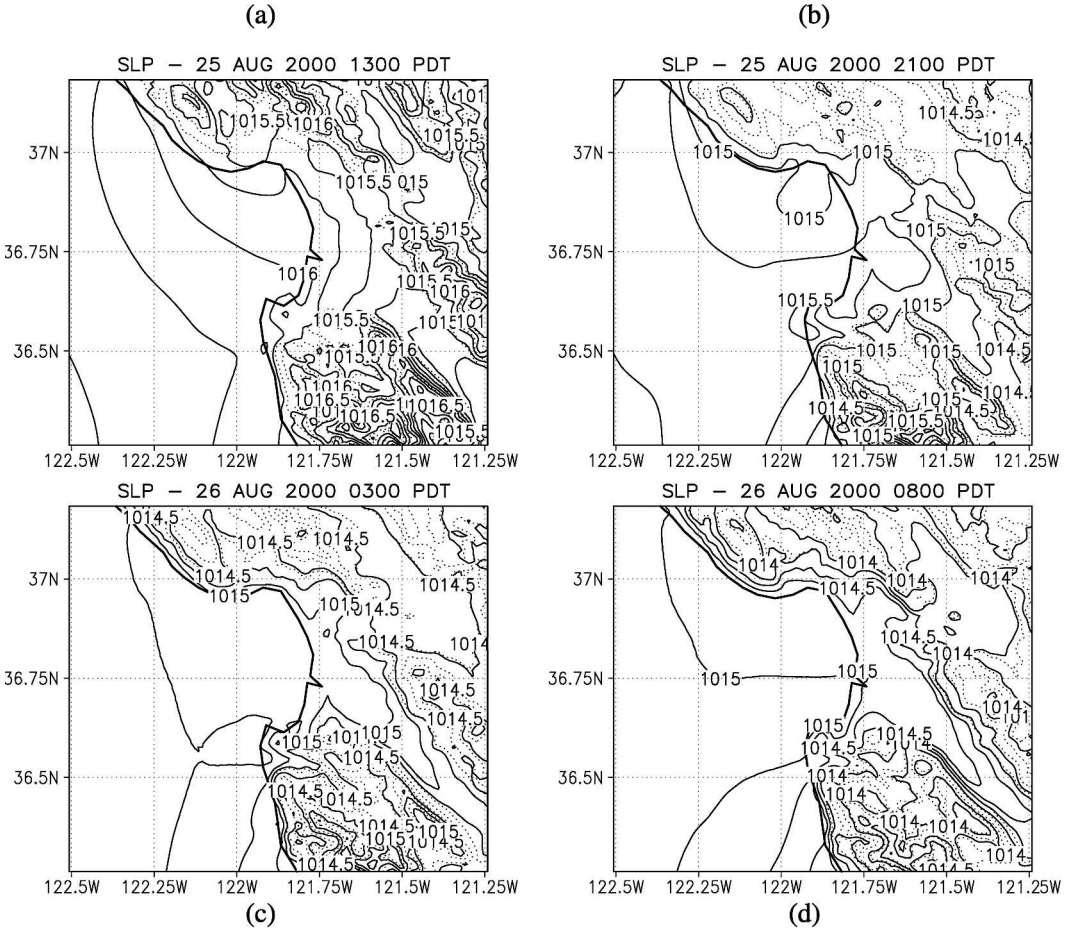

FIG. 4. Simulated sea level pressure (mb, solid line every 0.25 mb) on domain 2 during 25–26 Aug 2000 at key times of the SCE evolution: (a) sea breeze (1300 PDT); (b) mature stage of the first SCE occurrence (2100 PDT); (c) dissipating stage (0300 PDT); and (d) mature stage of the second SCE occurrence (0800 PDT). Terrain elevation is contoured with dotted lines every 200 m.

was stable, as potential temperature was increasing with height everywhere over water. Relative humidity (RH; instead of potential temperature) was thus used to identify the MBL as the layer with values of RH greater than 50% (not shown). It was found that the 296-K potential temperature contour could be used to determine approximately the top of the marine layer (or the bottom of the inversion) during the day. At night, the 292-K contour was a better choice.

Figure 7 shows that the marine layer was tilted upward over Monterey, due to the combination of two factors. First, the north-northwesterly flow entering Monterey Bay was blocked by the Monterey peninsula and forced to decelerate. Vertical motion was inhibited by the stable conditions and therefore cold, dense air converged over Monterey, causing the marine layer to rise. Second, the Santa Cruz area is protected from the cold north-northwesterly flow by the mountains to its north, and it is thus generally warmer and drier than the rest of the bay. Note also the upslope flow along the mountainside in Fig. 7a. The rising of warm air from the lower levels therefore caused the MBL to break down in the Santa Cruz area. The cross section shows that the high vertical vorticity shown previously in Fig. 2a originated at the surface, therefore suggesting that surface effects may be important for the eddy formation.

At the eddy onset, approximately 1900 PDT, the tilting of the marine layer was accentuated (Fig. 7b) and so was the thermal contrast between Santa Cruz and Monterey. Vorticity extended up to about 500 m and its maximum was still at the surface. Vertical motion, associated with wind convergence into the eddy center, extended up to 800 m, in opposition to the general subsiding motion noted earlier. Cooler air advected from the south had reached Santa Cruz, therefore causing temperature to decrease.

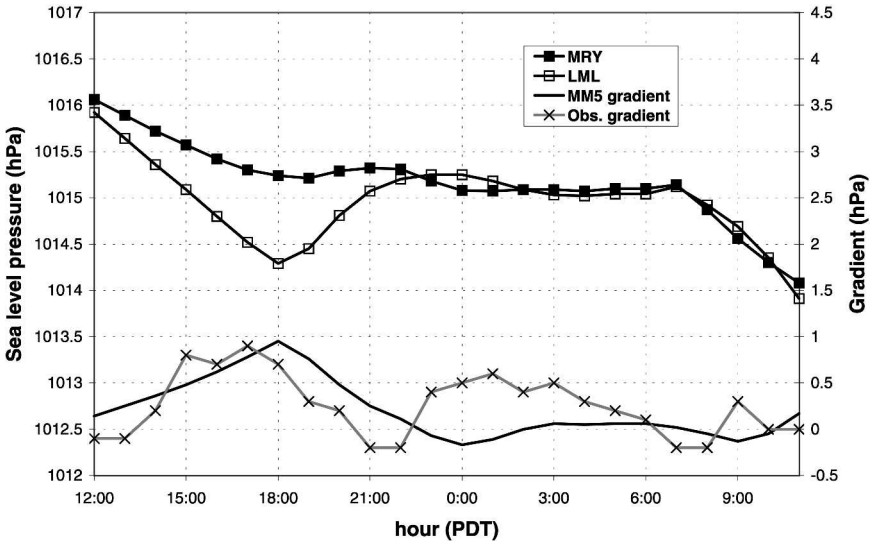

FIG. 5. Trends of simulated sea level pressure (hPa) at LML and MRY for 24 h starting at 1200 PDT on 25 Aug 2000. Observed and simulated south-to-north pressure gradients between the two stations are also plotted.

The homogenizing effect of the SCE can be noticed a few hours later, at 2100 PDT (Fig. 7c), when the temperature difference between south and north bay had almost disappeared. The SCE vorticity was continuously depleted as the eddy moved southward and the positive vertical velocity was limited to the lowest levels. In its fully developed stage, the eddy center had a temperature slightly warmer (~2°C) than its surroundings.

By 0300 PDT (not shown), the SCE had completely dissipated at all levels, although a pocket of its vorticity remained aloft at about 300 m. Temperature and mois-

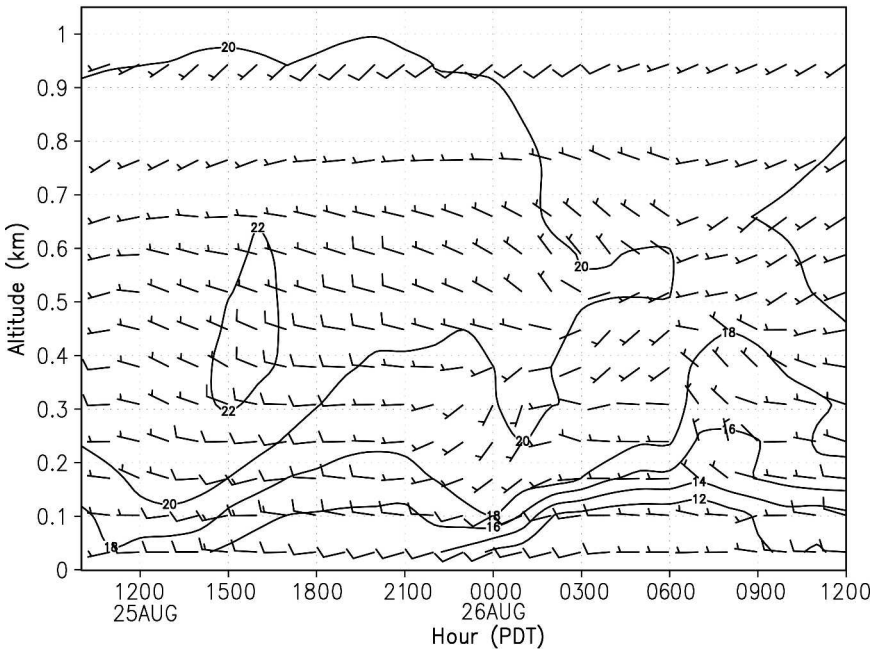

FIG. 6. Simulated wind barbs and virtual temperature (°C) at Fort Ord for 24 h starting at 1200 PDT on 25 Aug 2000, from ground level to 1-km elevation.

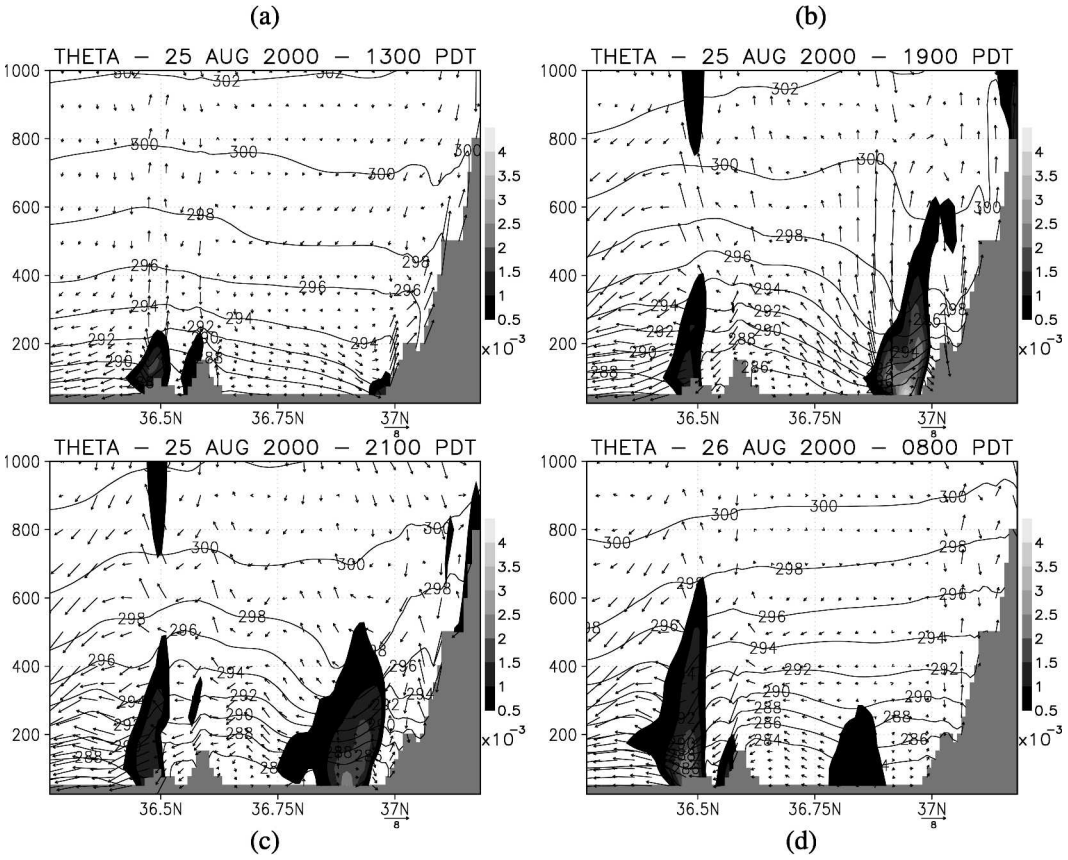

FIG. 7. North–south cross section of MM5 results for domain 2 during 25–26 Aug 2000 at key times of the SCE evolution: (a) sea breeze (1300 PDT); (b) onset of the first SCE occurrence (1900 PDT); (c) mature stage of the first eddy (2100 PDT); and (d) mature stage of the second SCE (0800 PDT). Terrain is shown with gray blocks. Vectors of wind components parallel to the section (i.e., v in m s^{-1} and w in cm s^{-1}) are shown together with vertical vorticity (10^{-3} s^{-1}, gray shaded) and potential temperature (K, solid line every 2 K).

ture fields were uniform everywhere over Monterey Bay. The second SCE eddy started forming slightly to the west of this cross section at this hour.

The mature stage of the second SCE (Fig. 7d) was characterized by smaller vertical extent (generally below 400 m), lower values of vorticity, and shorter lifetime (6 h as opposed to 9) than the first eddy. It also had a cool center and dissipated over water rather than over land, suggesting that the eddy dissipation is not necessarily caused by increased surface friction over land.

d. Summary of findings from the test case

It appeared from the surface and vertical analyses that the first/evening and the second/nocturnal eddies had different characteristics and formed in different ambient conditions. The first/evening eddy had higher vorticity, stronger vertical velocity, greater vertical extent and lasted longer than the second one. The first eddy had a homogenizing effect over the bay, by advecting cool and moist air from the south into the warmer and drier Santa Cruz. The second/nocturnal eddy instead formed in horizontally uniform temperature and moisture conditions. Moreover, the evening eddy had a warm core while the nocturnal eddy had a cooler center. However, they both formed in the Santa Cruz area and had a vertical profile of vorticity that decreased with height. Moreover, they both dissipated their vertical vorticity while moving southward after they detached from the SCM.

This suggests that the mechanism of formation may be the same for both eddies, but more favorable conditions in the late afternoon (e.g., south-to-north pressure gradient, stronger turning of the flow during the day, and upslope flow along the southern side of the Santa Cruz Mountains) make the evening/first eddy stronger and longer lasting. Since vorticity maxima are found in the same area (i.e., by Santa Cruz) where both

eddies initiate, finding the origin of the SCEs coincides with finding the origin of such vorticity.

3. Mechanisms of formation

In this section, possible sources of the vertical vorticity associated with the SCE formation are investigated through a sensitivity approach, in which one or more parameters (or physical components) are varied at a time.

The following possible factors and mechanisms of formation are discussed:

- Diabatic effects: the solar cycle is ultimately responsible for the south-to-north pressure gradient, the flow turning at the entrance of Monterey Bay, and the upslope flow along the south-facing sides of the Santa Cruz Mountains. By running MM5 with no solar cycle and no heat exchanges at the bottom level, such effects would be eliminated. No significant differences between first and second eddy should thus be found.
- Topography: the mountains to the north and to the south of Monterey Bay act as obstacles on the main northwesterly flow.
- Viscosity: the fact that vorticity maxima are found near the surface and that vorticity streaks emanate from the western side of the Santa Cruz Mountains suggest that the SCE could be formed by boundary layer separation, caused ultimately by internal and/or surface friction. Inviscid conditions would then prevent the SCE formation.
- Baroclinic mechanism: vertical vorticity can form in an inviscid and adiabatic flow past an obstacle, due to the tilting of horizontal vorticity generated by the solenoidal term.

Since these sensitivity runs have a rather large effect, results will be shown for a portion of domain 1 covering both San Francisco Bay and Monterey Bay. The base scenario, described in the previous section, will be referred to as "RUN1." The focus will be on vorticity formation. Vortex shedding and hydraulic jump dynamics will be analyzed in section 4.

a. Diabatic effects

According to Davis et al. (2000), diurnal heating is fundamental for the formation of the Catalina eddy. In their simulations with MM5, they showed that a stronger eddy would form if the ground was kept at its midday temperature. Vice versa, no eddy could form if the ground temperature was kept equal to its nocturnal value. Similarly, Wilczak et al. (1991) found that if diabatic heating were suppressed, the midchannel eddy would be weaker and the Gaviota eddy would not form at all. Diurnal effects were also invoked for the Auckland eddy by McKendry and Revell (1992). To verify the effect of diurnal cycle and heat exchange at the ground on the SCE, run "NOSUN" was carried out with the following settings:

- constant ground temperature (set equal to its initial value, representative of nocturnal conditions);
- no surface heat (and moisture) fluxes;
- no solar cycle (by setting the solar constant to a very small number).

In this run no substantial land heating occurred (Fig. 8), and therefore the pressure gradient force between ocean and land was greatly reduced (not shown). Consequently, no significant sea breeze formed in the afternoon and the main flow off the coast remained unchanged, that is, northwesterly. At 1500 PDT, an SCE was already fully developed (Fig. 9). This eddy was almost stationary throughout the night and it never dissipated. Vorticity was still formed along the western sides of the Santa Cruz Mountains, but did not reach values as high as it did in the test case (maxima were about 0.8×10^{-3} s^{-1} as opposed to 1.3×10^{-3} s^{-1} for RUN1). No upslope flow developed along the southern sides of the Santa Cruz Mountains (not shown).

In conclusion, the solar cycle was not a cause of the SCE events studied, since, after removing the solar cycle, the eddy still formed with approximately the same size and vorticity as the nocturnal SCE from the test case. The effect of the diurnal cycle was twofold. First, it destroyed the nocturnal eddy in the late morning, as surface heating was responsible for the sea breeze, which swept away the circulation associated with the SCE. Second, the diurnal cycle enhanced the evening eddy by increasing its vorticity due to the greater turning of the flow when the land is allowed to warm up and to the formation of a favorable south-to-north pressure gradient.

b. Topography

Two mountain chains are found in the Monterey Bay area: SCM, located to the northwest of the bay, and the Santa Lucia Mountains (SLM), located to the south of the bay (Fig. 1). To evaluate their effects on the SCE, the two chains were removed from both domains in separate runs, without SCM (run named "NOSCM") and without SLM ("NOSLM"). Land-use and soil parameters were not modified; a plateau of 10 m elevation replaced the original orography.

Without SCM, the SCE did not form at any time. At

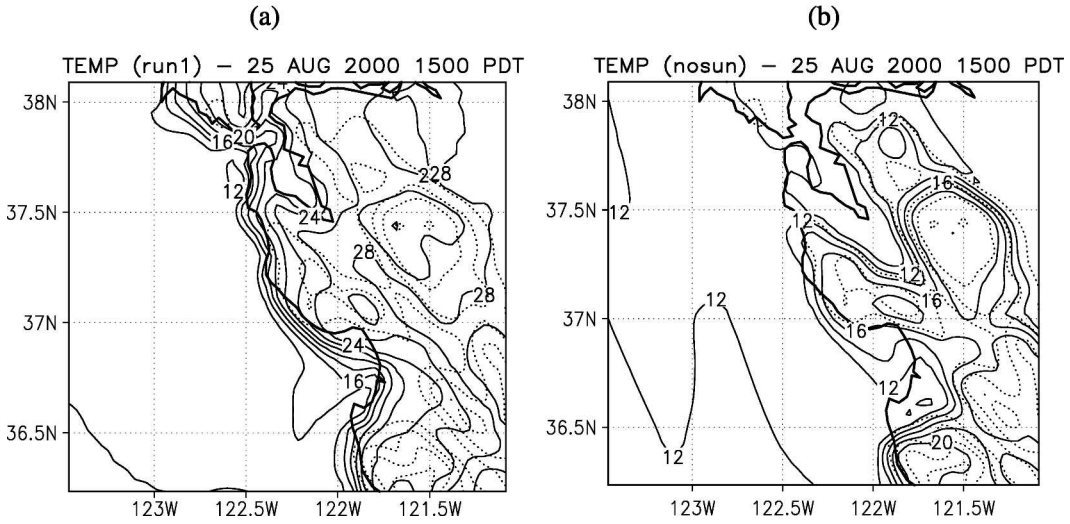

FIG. 8. Simulated temperature field (°C, solid line) and terrain elevation (m, dotted line) on domain 1 at 1500 PDT on 25 Aug 2000 from (a) RUN1 and (b) NOSUN.

2100 PDT, a large eddy was present over Monterey Bay as simulated by RUN1 and as confirmed by observations (Fig. 10a). However, simulated streamlines obtained with NOSCM at the same hour show no closed circulation, but rather a cyclonic turn of the flow in the Santa Cruz area, induced mainly by the blocking effect of the SLM to the south (Fig. 10b). Clearly, the SCM represent an obstacle to the main northwesterly flow, without which the SCE cannot form.

Without SCM, the entire peninsula from San Francisco to Santa Cruz was swept by a strong northwesterly flow in the afternoon (not shown). Surface friction still acted to reduce the wind speed over land and to slightly turn the flow into a more westerly direction, as expected for a system with high pressure to the west and low pressure to the east. Vertical vorticity still formed along the western flanks of the plateau, but less than in RUN1 (0.6×10^{-3} as opposed to 1.1×10^{-3} s^{-1}). A closed cyclonic circulation formed by the city of San Francisco for a few hours at about 0500 PDT (not shown), a San Francisco Eddy indeed!

The removal of the Santa Lucia Mountains in run NOSLM did not prevent the formation of the SCE, but it changed some of its characteristics. The first eddy formed farther to the east of Santa Cruz in NOSLM than in RUN1 (Fig. 11). Since the SLM blocking effect

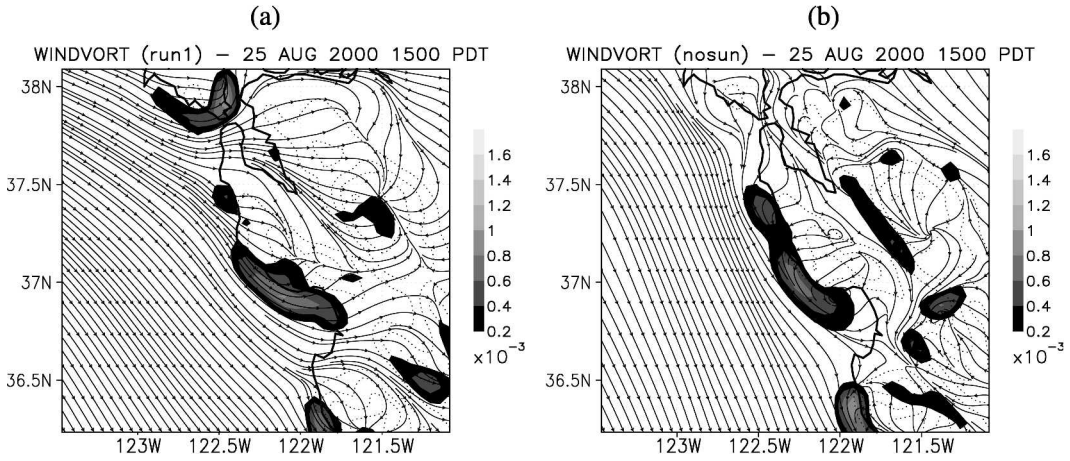

FIG. 9. Streamlines of simulated winds at the lowest sigma level and simulated vertical vorticity (10^{-3} s^{-1}, gray shaded) on domain 1 at 1500 PDT on 25 Aug 2000 from (a) RUN1 and (b) NOSUN. Terrain elevation is contoured with dotted lines every 200 m.

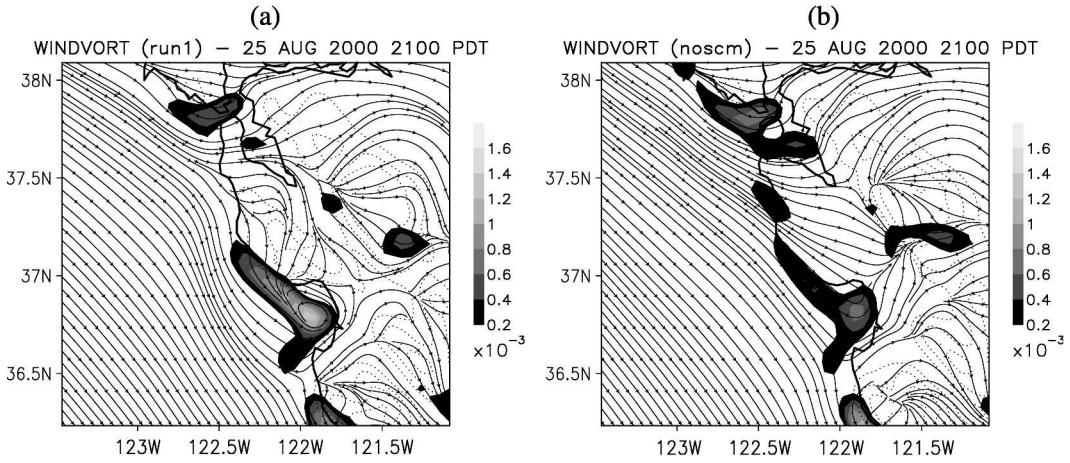

FIG. 10. Streamlines of simulated winds at the lowest sigma level and simulated vertical vorticity (10^{-3} s^{-1}, gray shaded) on domain 1 at 2100 PDT on 25 Aug 2000 from (a) RUN1 and (b) NOSCM. Terrain elevation is contoured with dotted lines every 200 m.

was missing, the main northwesterly flow entering Monterey Bay did not turn to a southwesterly direction as much as it did in RUN1. As a consequence, the eddy was confined to the eastern part of the bay and had a more elongated shape, with the symmetry axis parallel to the mean flow. Furthermore, less vorticity was created, since less turning of the flow occurred. In general, wind speeds were higher everywhere without SLM (not shown). In particular, the expansion fan was so much larger in NOSLM that it occupied most of the bay. The first SCE never detached and quickly dissipated by 2200 PDT. A second eddy formed at about 0200 PDT and lasted until 0900 PDT (not shown). Since the expansion fan lasted longer in NOSLM, the second SCE too was confined to the northeastern corner of Monterey Bay and had the same elongated and twisted axis as the first one. No detachment occurred for the second SCE instance either. This suggests that the elimination of the SLM effectively suppressed vortex shedding.

In summary, topography dramatically affected the SCE. The SCM are necessary for the eddy formation: without them, no obstacle interacts with the main northwesterly flow and not enough vorticity forms. The SLM are not necessary for the SCE formation, but they affect its shape and duration. Without them, the eddy is confined to the northwestern part of Monterey Bay, it has a more elongated shape, and no vortex shedding occurs.

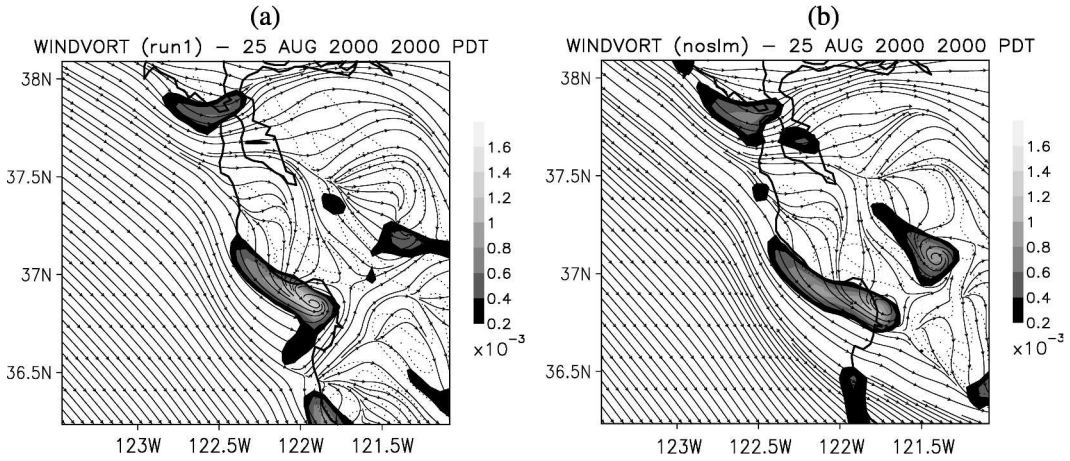

FIG. 11. Streamlines of simulated winds at the lowest sigma level and simulated vertical vorticity (10^{-3} s^{-1}, gray shaded) on domain 1 at 2000 PDT on 25 Aug 2000 from (a) RUN1 and (b) NOSLM. Terrain elevation is contoured with dotted lines every 200 m.

c. Viscosity

In general, the mean kinetic energy directly dissipated by molecular viscosity is negligible compared with that dissipated by turbulent (or eddy) viscosity. For this reason, molecular viscosity is ignored in MM5, but eddy viscosity is not. The MM5 system is still viscous because the dissipative effect of viscosity is included in the eddy friction term. A truly inviscid system is one in which both molecular and eddy viscosities and surface friction between air and the ground are zero. Surface friction can be removed by setting, for example, a free-slip boundary condition, as opposed to a viscous no-slip condition. Surface friction is not a separate physical process but a manifestation of the flow viscosity at the fluid/solid interface.

The literature related to flow past an obstacle is vast and is only briefly described here. The fact that more than one SCE formed and moved southward brings to mind the von Kármán vortex streets in two-dimensional, homogeneous, viscous flow past a cylinder (Kundu 1990). For such flow, a wake with a pair of stationary, counterrotating vortices forms when the Reynolds number [$\mathrm{Re} = (VD/\upsilon)$, where V is the upstream velocity, υ the kinematic viscosity, and D the cylinder diameter] is greater than four; the wake breaks into an oscillating Kármán vortex street if $\mathrm{Re} > 40$ (Kundu 1990, p. 321). Laboratory studies too have attributed the formation of lee vortices downstream of three-dimensional obstacles to the separation of the viscous boundary layer from the lower surface (Brighton 1978; Hunt and Snyder 1980; Castro et al. 1983; Snyder et al. 1985). The extension of the boundary layer separation theory from homogeneous to stratified flows was first proposed by Chopra and Hubert (1965). Even though subsequent studies (discussed in the next section) have proven that boundary layer separation is not necessary for eddy formation in stratified flows, the effect of viscosity on the SCE is still studied here from the point of view of the vorticity equation:

$$\frac{d\boldsymbol{\omega}}{dt} = \underbrace{(\boldsymbol{\omega}\cdot\boldsymbol{\nabla})\mathbf{u}}_{\text{tilting/stretching}} - \overbrace{\boldsymbol{\omega}(\boldsymbol{\nabla}\cdot\mathbf{u})}^{\text{divergence}} - \underbrace{\boldsymbol{\nabla}\left(\frac{1}{\rho}\right)\times\boldsymbol{\nabla}p}_{\text{solenoidal}} + \overbrace{\boldsymbol{\nabla}\times(\upsilon\nabla^2\mathbf{u})}^{\text{molec. viscosity}} + \underbrace{\boldsymbol{\nabla}\times\mathbf{F}'}_{\text{eddy viscosity}}, \tag{2}$$

where $\mathbf{u} = u\mathbf{i} + \upsilon\mathbf{j} + w\mathbf{k}$ is the three-dimensional wind vector, ρ is density, p is pressure, $\boldsymbol{\omega}$ is absolute vorticity, ν is molecular viscosity, and $\mathbf{F}'$ is eddy friction. Note that, only for incompressible flows with uniform and constant υ, the molecular viscosity term can be rewritten as $\upsilon\nabla^2\boldsymbol{\omega}$ and thus molecular viscosity can only diffuse vorticity. For compressible flows, with the irrotational and barotropic assumptions [i.e., all terms on right hand side of Eq. (2) are zero except for the last one], vorticity can still be generated by the curl of eddy friction, that is, by horizontal and/or vertical wind speed gradients. Haynes and McIntyre (1987) and Schär and Smith (1993a) introduced a "dissipative flux" to express the same concept. Grubišić et al. (1995) found that vorticity production by the dissipative flux was negligible away from regions with horizontal variations of either fluid depth or surface roughness. Epifanio and Durran (2002b) found little contribution of eddy viscosity to the wake vorticity generation.

The importance of viscosity on the SCE was investigated in run NOPBL, where no turbulence parameterization was used (thus no eddy viscosity) and where a free-slip condition was forced at the surface (thus no surface friction). Consequently, no momentum, heat, or moisture fluxes were allowed in the domains, neither at the surface nor aloft. Ground temperature was kept constant too. To maintain numerical stability, a horizontal diffusion term is present in MM5 (Grell et al. 1994). Since the horizontal diffusion operator is applied on sigma surfaces, it could potentially generate vertical diffusion and dissipation and thus violate the inviscid constraint. On one hand, this effect was found to be negligible in an earlier version of MM5 (Kuo et al. 1988). Numerical diffusion was added also in Schär and Smith (1993a) to smooth fields, but it did not affect the inviscid nature of their results (away from jumps). On the other hand, Vosper (2000) found a large effect of numerical viscosity in another numerical model with the sigma-pressure coordinate. Some numerical viscosity was found in MM5 in this study also, as discussed in section 4. However, for the purpose of this discussion, the settings imposed on MM5 made the system as close to inviscid as technically possible.

Great differences between the results obtained with NOPBL and the test case can be noticed already in the afternoon. Since the ground was not allowed to warm up during the day, and since no surface fluxes could exchange heat between air and soil, the temperature difference between ocean and land was much lower in NOPBL (not shown). Consequently, the pressure gradient between ocean and land was reduced and therefore the main flow over Monterey Bay was weaker and less westerly in NOPBL than in the test case (Figs. 12a,b). Since the flow was weaker, winds were affected more by local features, such as valleys or slopes, in NOPBL. An SCE had already formed at noon; since it formed within weaker synoptic forcing, the eddy was larger in the horizontal than under normal conditions.

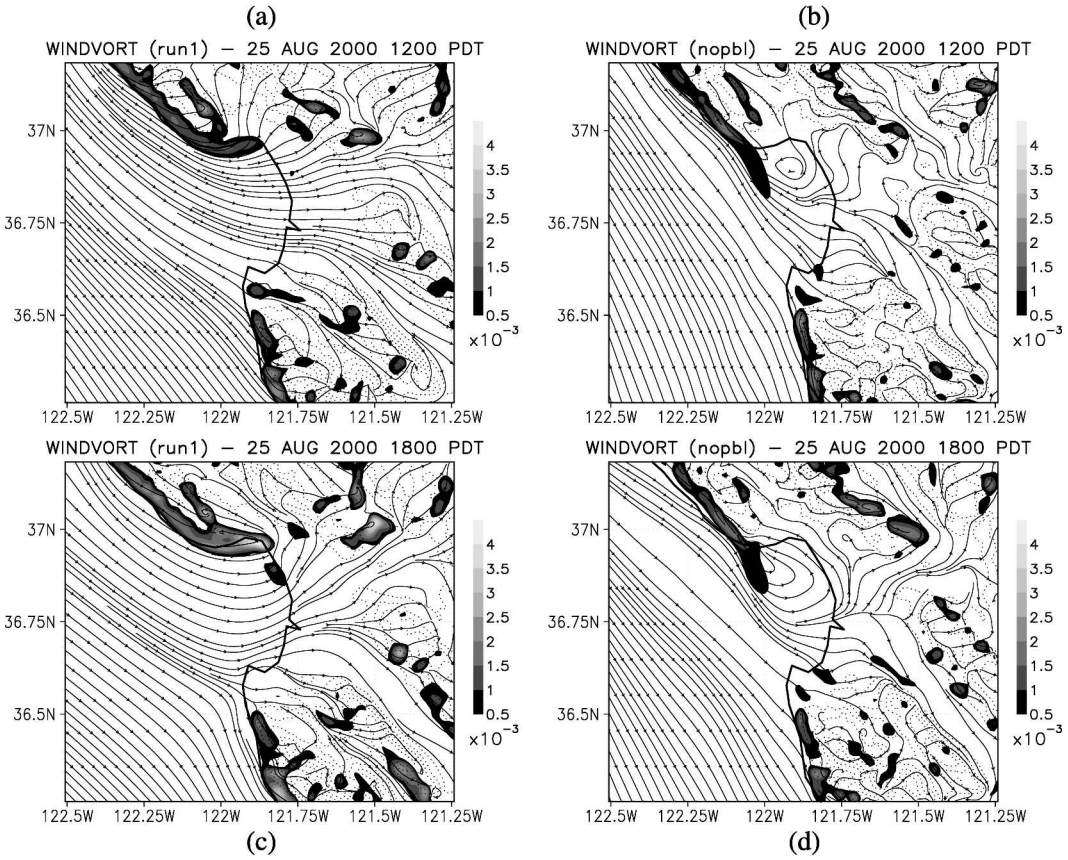

FIG. 12. Streamlines of simulated winds at the lowest sigma level and simulated vertical vorticity (10^{-3} s^{-1}, gray shaded) on domain 2 at 1200 and 1800 PDT on 25 Aug 2000 from (left) RUN1 and (right) NOPBL. Terrain elevation is contoured with dotted lines every 200 m.

No expansion fan formed offshore from Santa Cruz and therefore vorticity was generally lower in run NOPBL (Figs. 12c,d). The first SCE detached at 0100 and dissipated by 0300 PDT, but a second eddy formed an hour later. This SCE was more elongated and narrow than the corresponding one in the test case (not shown); it continued until 0900 PDT but it never detached. A third eddy started at about 1000 PDT on 26 August (not shown). All eddies had a smaller vertical size than in the test case.

In conclusion, the mixing of momentum and heat produced by turbulent friction does not appear to be a fundamental mechanism for the SCE formation, but it affects several details of its evolution. With no friction, an SCE still formed on the south side of the SCM. However, it was characterized by weaker winds and vorticity, a more elongated shape, and smaller vertical development than in the test case. Furthermore, multiple instances of the SCE formed throughout the 2-day period, regardless of the time of the day, due to the absence of heat or momentum fluxes at all levels, which would have otherwise dissipated the eddy during the day. Vortex shedding was almost suppressed, as only one eddy (the first one) detached from the SCM. This may appear surprising, as a decrease in friction should enhance vortex shedding rather than suppress it (Grubišić et al. 1995; Vosper 2000). However, the reversed flow in the wake is weaker in the inviscid case and consequently wake instability and vortex shedding are less likely to develop. Overall, it can be concluded that frictional generation of vorticity in the SCE case is greater than frictional dissipation.

d. Baroclinic mechanism

Modeling studies have first shown that, in three-dimensional stratified flow, vortices would intensify when surface friction was either reduced (Wilczak and Glendening 1988) or removed (Smolarkiewicz et al. 1988; Kuo et al. 1988). As such, the analogy between vortex street in homogeneous flow and vortex shedding in stratified flow was compromised. It was only a year later that Smolarkiewicz and Rotunno (1989a) pro-

posed a new vorticity formation mechanism for inviscid, stratified flow past a three-dimensional obstacle, namely the baroclinic mechanism. To illustrate it, the vorticity vector is split here into its vertical (ζ) and horizontal ($\boldsymbol{\omega}_h$) components, which both satisfy the inviscid vorticity equation [Eq. (2)] as follows:

$$\frac{d\zeta}{dt} = (\boldsymbol{\omega} \cdot \boldsymbol{\nabla})w - \zeta(\boldsymbol{\nabla} \cdot \mathbf{u}) - \mathbf{k} \cdot \boldsymbol{\nabla}\left(\frac{1}{\rho}\right) \times \boldsymbol{\nabla} p, \quad (3)$$

$$\frac{d\boldsymbol{\omega}_h}{dt} = (\boldsymbol{\omega} \cdot \boldsymbol{\nabla})\mathbf{u}_h - \boldsymbol{\omega}_h(\boldsymbol{\nabla} \cdot \mathbf{u}) + \left[-\boldsymbol{\nabla}\left(\frac{1}{\rho}\right) \times \boldsymbol{\nabla} p \right]_h, \quad (4)$$

where the subscript h indicates a horizontal component. The tilting/stretching and divergence terms would all be zero in an initially irrotational system (i.e., in which $\boldsymbol{\omega} = 0$ at $t = 0$), since vorticity appears in them as a multiplying factor. The last term, called "solenoidal" or "baroclinic," is the only one that could from vorticity.

The solenoidal term is zero in barotropic flows by definition. However, its effect in Eq. (3) is negligible even in baroclinic flows, therefore suggesting that vertical vorticity cannot be directly generated inviscidly. This is not entirely accurate. As shown first by Smolarkiewicz and Rotunno (1989a) for a simplified system (anelastic, adiabatic, Boussinesq, and hydrostatic), the solenoidal term is not negligible in Eq. (4), and it can therefore create horizontal vorticity. Once $\boldsymbol{\omega}_\mathrm{h}$ becomes nonzero, the tilting/stretching term in Eq. (3) becomes nonzero too and thus vertical vorticity can be generated. Note that no assumption, besides inviscid flow, was made so far.

By imposing a free-slip boundary condition in their numerical simulations, Smolarkiewicz and Rotunno (1989a) effectively prevented the formation of a boundary layer and yet obtained a pair of vortices for the range $0.1 < \mathrm{Fr} < 0.5$. After their seminal study, several other studies have confirmed the validity of the baroclinic mechanism (Smolarkiewicz and Rotunno 1989b; Rotunno and Smolarkiewicz 1991; Schär and Durran 1997; Rotunno et al. 1999; Vosper 2000). Kuo et al. (1988) and Wilczak and Glendening (1988) found that surface friction acted as a sink, rather than a source, of vorticity for the case of a mesoscale vortex that formed over China and for the Denver Cyclone, respectively. Also, Crook et al. (1990) found no significant differences between runs with and without surface friction; similarly, Grubišić et al. (1995) showed that surface friction is not the dominant vorticity formation mechanism in shallow-water flows past an obstacle, but it interferes with vortex shedding by making the wake more stable.

To investigate the importance of the baroclinic mechanism and the ultimate causes of the solenoidal term, it was necessary to run a simulation as close as possible to adiabatic conditions. Since MM5 is not suitable for idealized runs (Chuang and Sousonis 2000), fully adiabatic and inviscid conditions cannot be achieved during the simulations. The best solution was to use the same conditions as in NOSUN, but with neither a turbulence parameterization nor surface friction, to make the flow inviscid. Since the solenoidal term could be theoretically forced by a spatial gradient in (potential) temperature (Pielke and Segal 1986), the initial temperature of ground and water was set uniform to a constant value of 14°C (from this the run was named "UNIF"). Note, however, that temperature, pressure, and density in the initial conditions were still the same as those in the test case, and therefore they were inconsistent with the horizontally homogeneous temperature field imposed at the ground. Note also that the initial wind field was not irrotational but contained some vertical vorticity and potential vorticity, which were in the initial conditions. Even with these limitations, results from run UNIF were useful for identifying the origin of the solenoidal term.

With run UNIF, not only did the eddy still form, but it also had characteristics very similar to those from run NOPBL, except for a time lag of 6 h, explained by the lack of a diurnal cycle. In addition, no vortex shedding occurred throughout this simulation. Without any friction/turbulence and without any diabatic effects, the horizontal contours of vertical vorticity (Fig. 13a) show again the typical streaks emanating from the sides of the Santa Cruz Mountains, also obtained for example by Schär and Durran (1997), Schär and Smith (1993a), Crook et al. (1990, 1991).

An analysis of the relative importance of all four terms of the vorticity equation in the vertical was performed at 0200 PDT, when the first eddy had formed. In general, the greatest magnitudes are given by the tilting/stretching and the advection terms (not shown). The tilting/stretching, however, is the only term with a significant contribution at the entrance of Monterey Bay (Fig. 13b), where vorticity maxima were found.

In the horizontal, no term has a significant contribution at the entrance of Monterey Bay except for the solenoidal term, which is greatly affected by the presence of the SCM (Fig. 13c). In fact, at all times, the horizontal solenoidal vectors rotate clockwise around the SCM, a pattern consistent with that of the horizontal vorticity vector in Smolarkiewicz and Rotunno (1989b, their Figs. 1f and 1i), Crook et al. (1990, their Fig. 13), and Schär and Durran (1997, their Fig. 11).

4. Other remarks

In this section, other factors affecting the SCE are investigated.

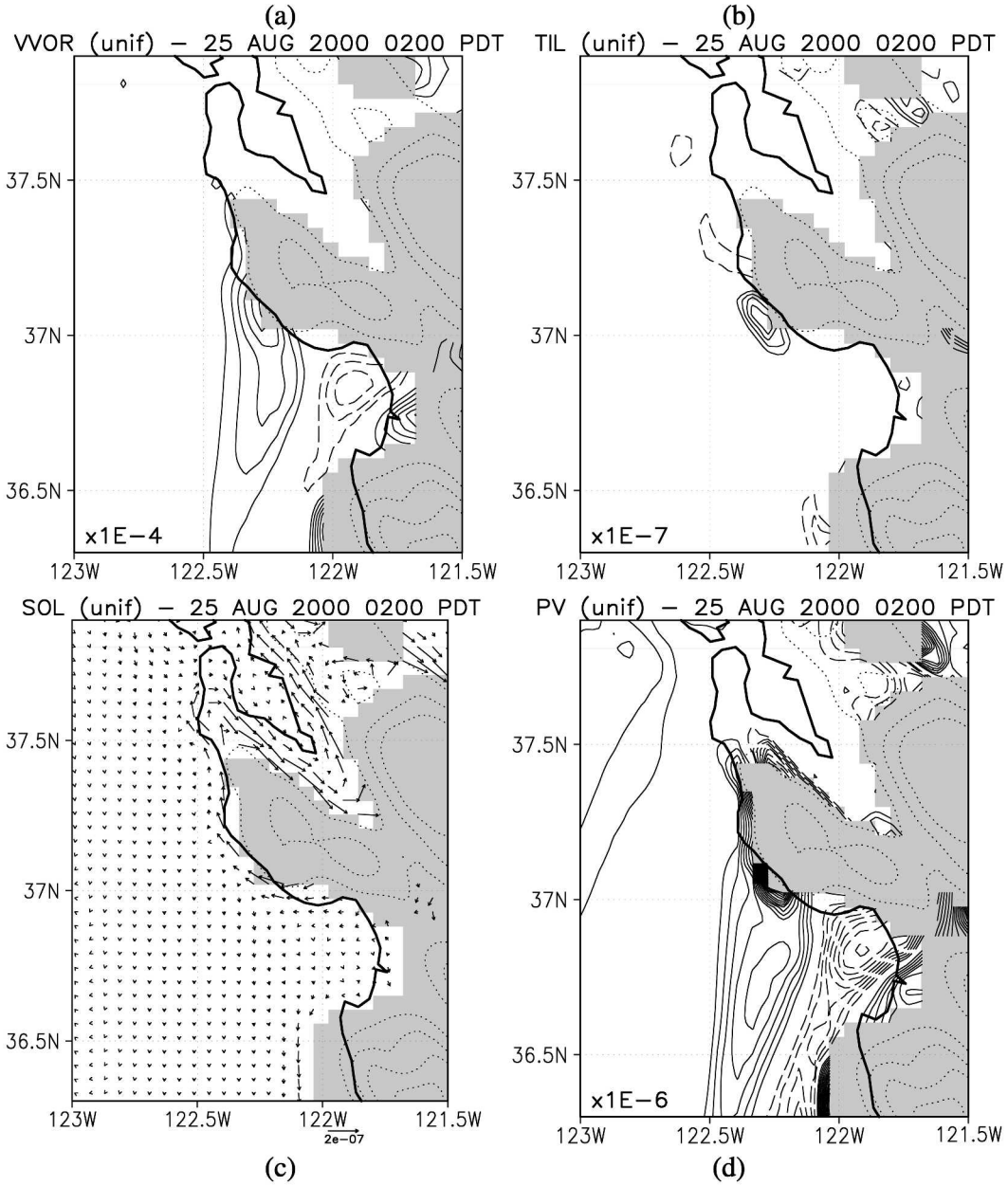

FIG. 13. Fields from run UNIF on isentropic surface $\theta = 292$ K, pierced by the Santa Cruz Mountains where shaded, at 0200 PDT on 25 Aug 2000; (a) vertical vorticity (s^{-1}); (b) tilting (s^{-1}); (c) horizontal solenoidal vector; and (d) potential vorticity (K m^2 s^{-1} kg^{-1}). Contour interval is shown on each panel; negative values are long dashed. Terrain is contoured with dotted lines every 200 m.

a. Inversions

The importance of an elevated inversion was first suggested by Hubert and Krueger (1962). In their study, several aspects of vortex streets observed on the lee of the Canary Islands were consistent with inertial oscillations or inertial instabilities for stable and unstable wakes respectively. The presence of an inversion is then favorable because it increases lateral mixing and consequently triggers stronger inertial oscillations. Chopra (1973) hypothesized that the presence of an inversion at half height of the mountain is necessary for the formation of a vortex street. In fact, surveys of sounding data confirm that most vortices form where a sharp inversion is located below the obstacle crest (Epifanio and Rotunno 2005). The stability of the inversion

causes upstream flow blocking and consequent deflection around, rather than over, the obstacle. In other words, an inversion would reduce the Fr of the flow. Moreover, the phase diagram in Schär and Smith (1993a, their Fig. 3) shows that a wake with reversed flow always forms when the mountain height is greater than the fluid depth within the shallow-water approximation. Consistently, it was found in Archer and Jacobson (2005) that the SCE was more likely to form when the marine layer was lower than 500 m, that is, when the inversion was located below the top of the Santa Cruz Mountains. However, sensitivity runs without viscosity or without diurnal cycle showed that the baroclinic mechanism could act even without an inversion, in almost isothermal conditions (not shown). Nonetheless, the presence of the inversion is favorable to eddy formation because it prevents the main north/northwesterly flow from going over the Santa Cruz Mountains, and therefore it precludes any downslope flow from interfering with the SCE formation. Since a marine inversion over central California is most common in the summer, the summertime nature of the SCE can be partially explained. Also, the baroclinic mechanism acts preferentially in the summer, when strong and steady north/northwesterly flow, typical of the central California coast, interacts with the Santa Cruz Mountains. This same north/northwesterly flow also impinges against the Santa Lucia Mountains to the south of Monterey Bay, contributing to the local south-to-north pressure gradient that strengthens the SCE in the afternoon.

b. Hydraulic jumps

Another mechanism of vorticity formation for stratified flow past an obstacle is through discontinuities, such as hydraulic jumps. Schär and Smith (1993a) showed that, within the shallow-water approximation, a hydraulic jump and a wake with reversed flow (i.e., vortex pairs) can form inviscidly when the obstacle pierces through the fluid depth. Dissipation, however, occurred at the jump via jump conditions; as such, this system was defined as "pseudoinviscid." Epifanio and Durran (2002a) found similar jump features in numerical simulations of free-slip, laminar, and viscous flow. Via a Lagrangian vorticity decomposition with propagator matrices, Epifanio and Durran (2002b) were able to conclude that the role of hydraulic jumps is to amplify baroclinically generated vorticity via stretching. Since a region of supercritical flow was found at the entrance of Monterey Bay for the SCE eddy case (see Fig. 3), the presence of a hydraulic jump is expected somewhere over the bay. Burk and Haack (2000) have in fact documented the formation of cloud bands associated with a shock feature over Monterey Bay. However, no striking evidence of its existence was found in RUN1 from either domain. Regardless, runs NOPBL and UNIF showed vortex formation with no sign of supercritical flow upstream of the bay. Consequently, vorticity formation via a hydraulic jump does not appear fundamental in the SCE case.

c. Potential vorticity

Another aspect of relevance to vortex formation is potential vorticity, defined as

$$\Pi = \frac{\boldsymbol{\omega}}{\rho} \cdot \boldsymbol{\nabla}\theta. \tag{5}$$

From Pedlosky (1987) and following Haynes and McIntyre (1987), the potential vorticity equation can be written as

$$\frac{d\Pi}{dt} = \boldsymbol{\nabla} \cdot \left(\frac{\Psi\boldsymbol{\omega}}{\rho}\right) - \boldsymbol{\nabla} \cdot \left(\frac{\boldsymbol{\nabla}\theta}{\rho} \times \frac{\mathbf{F}_d}{\rho}\right) = -\boldsymbol{\nabla} \cdot \mathbf{J}, \tag{6}$$

where Ψ includes conductive and diabatic effects, F_d is friction (due to molecular and/or eddy viscosity), and $\mathbf{J}$ is the dissipative vector:

$$\mathbf{J} = -\frac{\Psi\boldsymbol{\omega}}{\rho} - \frac{\mathbf{F}_d}{\rho} \times \frac{\boldsymbol{\nabla}\theta}{\rho}. \tag{7}$$

Potential vorticity can therefore be formed (destroyed) due to the convergence (divergence) of the dissipative vector, consisting of the sum of frictional and diabatic effects. In adiabatic and inviscid flow, therefore, potential vorticity is conserved. For an initially irrotational flow, the vorticity vector must lie on isentropic surfaces at all times. In UNIF, Π is thus expected to be relatively small and uniform along the sides of the SCM. However, Fig. 13d shows appreciable potential vorticity on the 292-K isentrope right where vorticity steaks formed. Similarly, nonexact potential vorticity conservation was also obtained by Smolarkiewicz and Rotunno (1989a) in "regions where the θ surfaces lowered to the point of intersecting the lower boundary of the model." Skamarock et al. (2002) also found potential vorticity anomalies on the leading edges of a simulated Catalina eddy, but they concluded that Π did not play a significant role in vortex formation. Since no diabatic effects are possible without solar radiation, the only explanation for potential vorticity in run UNIF is the inevitable numerical viscosity present in the MM5. Similarly, Vosper (2000, his Fig. 12) found that numerical viscosity was causing large vorticity normal to the isentropes.

d. Vortex shedding

The final aspect to investigate is vortex shedding. In homogeneous flows, the transition from a stationary vortex pair to vortex shedding is achieved by simply increasing Re past a critical value (~40). Sun and Chern (1994), however, did not obtain vortex shedding in their simulations of stratified flow past an isolated mountain for $1 < \mathrm{Re} < 1000$, therefore suggesting that a critical Re might not exist for vortex shedding in stratified flow. It was only by introducing some asymmetries (such as Coriolis rotation, wind perturbations, or asymmetric obstacle shapes) that they achieved vortex shedding. Analogously, Schär and Smith (1993b) obtained vortex shedding by suppressing a symmetry condition previously imposed in their method of calculation (Schär and Smith 1993a). By studying the evolution of the most unstable normal mode in a pseudoinviscid shallow-water system, they proved that vortex shedding was induced by a nonlinear oscillation that became perfectly periodic (sinusoidal) in time, thus causing the shed vortices to align in a perfectly periodic wake. They concluded that global instability of the wake was causing vortex shedding.

An analysis of the wake instability for the SCE case is beyond the scope of this study. However, several conclusions can be drawn from the results discussed. First, the geometry of the SCM and the flow around them are nonsymmetric, thus suggesting that the simulated vortex shedding (RUN1) is realistic. However, such asymmetric conditions persist in all sensitivity runs, but vortex shedding is suppressed in most of them. For example, the removal of the diurnal cycle prevented vortex shedding. This is possibly consistent with Sun and Chern (1993), who found that the removal of the diurnal cycle doubled the period of vortex shedding. Asymmetries therefore do not appear to be sufficient for SCE shedding. Second, vortex detachment occurred with and without viscosity, therefore suggesting that friction is not a critical factor for shedding in the SCE case. Furthermore, two out of three inviscid eddies were stationary. This was somewhat counterintuitive, as Grubišić et al. (1995) found that surface friction was not only reducing the size and strength of the wake, but also preventing vortex shedding by making the wake more stable. Their findings are consistent with observations, as atmospheric vortex shedding has been observed mainly over water in the wakes of islands (Hubert and Krueger 1962; Chopra and Hubert 1965; Smolarkiewicz et al. 1988; Sun and Chern 1993), which have lower surface roughness compared to wakes over land. To the authors' knowledge, no vortex shedding has been observed in the lee of orographic barriers over land, or past capes or bays over water (except for the SCE). The effect of friction on the SCE shedding appears to be the opposite of that on shallow-water flows in that frictional generation of vorticity dominates frictional dissipation. Further investigations are needed to fully elucidate this aspect.

5. Summary and conclusions

The SCE formation is rather complex, since it involves four different mechanisms acting together. The baroclinic theory, inspired by the findings of Smolarkiewicz and Rotunno (1989a), appears to be the fundamental mechanism for vertical vorticity formation. The solenoidal term, directly related to a fluid change in pressure not accompanied by a density adjustment, creates horizontal vorticity along the Santa Cruz Mountains' sides. The tilting/stretching term then acts to tilt the horizontal vorticity into the vertical, creating the vertical vorticity necessary for the formation of a vortex downstream.

Friction represents an additional source of vorticity, related to the fact that viscous dissipation is present in the turbulent airflow and that velocity has to be null at the surface along the mountainsides. This wind shear, perpendicular to the sloped terrain, causes both horizontal and vertical vorticity. These two mechanisms (i.e., solenoidal and frictional) act both during the day and night.

During the day only, two other mechanisms form vertical vorticity. First, the sea breeze forces a westerly flow over Monterey Bay and southerly flow to the east of Santa Cruz, causing an expansion fan at the entrance of the bay. Vorticity is therefore formed there as a result of both flow turning and horizontal wind shear. Finally, favorable conditions for a flow reversal (i.e., against the main northwesterly winds) are created in the afternoon by the south-to-north pressure gradient, which forces flow down the gradient from the south of Monterey Bay toward Santa Cruz.

Acknowledgments. This work was supported by the National Science Foundation (NSF) and by the National Aeronautics and Space Administration (NASA). The MM5 preprocessors were run at NCAR, which also provided data for the initial conditions. Constructive comments from an anonymous reviewer are gratefully acknowledged.

REFERENCES

Archer, C. L., 2004: The Santa Cruz eddy and U.S. wind power. Ph.D. thesis, Stanford University, 190 pp.

——, and M. Z. Jacobson, 2005: The Santa Cruz eddy. Part I: Observations and statistics. *Mon. Wea. Rev.,* **133,** 767–782.

Brighton, P. W., 1978: Strongly stratified flow past three-dimensional obstacles. *Quart. J. Roy. Meteor. Soc.,* **104,** 289–307.

Burk, S. D., and T. Haack, 2000: The dynamics of wave clouds upwind of coastal topography. *Mon. Wea. Rev.,* **128,** 1438–1455.

——, ——, and R. M. Samelson, 1999: Mesoscale simulation of supercritical, subcritical, and transitional flow along coastal topography. *J. Atmos. Sci.,* **56,** 2780–2795.

Castro, I. P., W. H. Snyder, and G. L. Marsh, 1983: Stratified flow over three-dimensional ridges. *J. Fluid Mech.,* **135,** 261–282.

Chen, F., and Coauthors, 1996: Modeling of land surface evaporation by four schemes and comparison with FIFE observations. *J. Geophys. Res.,* **101D,** 7251–7268.

——, Z. Janjić, and K. Mitchell, 1997: Impact of atmospheric surface-layer parameterizations in the new land-surface scheme of the NCEP mesoscale ETA model. *Bound.-Layer Meteor.,* **85,** 391–421.

Chopra, K. P., 1973: Atmospheric and oceanic flow problems introduced by islands. *Advances in Geophysics,* Vol. 16, Academic Press, 297–421.

——, and L. F. Hubert, 1965: Mesoscale eddies in wake of islands. *J. Atmos. Sci.,* **22,** 652–657.

Chuang, H.-Y., and P. J. Sousonis, 2000: A technique for generating idealized initial and boundary conditions for the PSU–NCAR model MM5. *Mon. Wea. Rev.,* **128,** 2875–2882.

Crook, N. A., T. L. Clark, and M. W. Moncrieff, 1990: The Denver Cyclone. Part I: Generation in low Froude number flow. *J. Atmos. Sci.,* **47,** 2725–2742.

——, ——, and ——, 1991: The Denver Cyclone. Part II: Interaction with the convective boundary layer. *J. Atmos. Sci.,* **48,** 2109–2126.

Davis, C., S. Low-Nam, and C. F. Mass, 2000: Dynamics of a Catalina eddy revealed by numerical simulation. *Mon. Wea. Rev.,* **128,** 2885–2904.

Dudhia, J., 1993: A nonhydrostatic version of the Penn State/NCAR mesoscale model: Validation tests and simulation of an Atlantic cyclone and cold front. *Mon. Wea. Rev.,* **121,** 1493–1513.

Epifanio, C. C., and D. R. Durran, 2002a: Lee-vortex formation in free-slip stratified flow over ridges. Part I: Comparison of weakly nonlinear inviscid theory and fully nonlinear viscous simulations. *J. Atmos. Sci.,* **59,** 1153–1165.

——, and ——, 2002b: Lee-vortex formation in free-slip stratified flow over ridges. Part II: Mechanisms of vorticity and PV formation in nonlinear viscous wakes. *J. Atmos. Sci.,* **59,** 1166–1181.

——, and R. Rotunno, 2005: The dynamics of orographic wake formation in flows with upstream blocking. *J. Atmos. Sci.,* in press.

Grell, G. A., J. Dudhia, and D. R. Stauffer, 1994: A description of the fifth-generation Penn State/NCAR Mesoscale Model (MM5). NCAR Tech. Note NCAR/TN-398+STR, National Center for Atmospheric Research, Boulder, CO, 121 pp.

Grubišić, V., R. B. Smith, and C. Schär, 1995: The effect of bottom friction of shallow-water flow past an isolated obstacle. *J. Atmos. Sci.,* **52,** 1985–2005.

Haack, T., S. D. Burk, C. Dorman, and D. Rogers, 2001: Supercritical flow interaction within the Cape Blanco–Cape Mendocino orographic complex. *Mon. Wea. Rev.,* **129,** 688–708.

Haynes, P. H., and M. E. McIntyre, 1987: On the evolution of vorticity and potential vorticity in the presence of diabatic heating and frictional or other forces. *J. Atmos. Sci.,* **44,** 828–841.

Hsie, E.-Y., R. A. Anthes, and D. Keyser, 1984: Numerical simulation of frontogenesis in a moist atmosphere. *J. Atmos. Sci.,* **41,** 2581–2594.

Hubert, L. F., and A. F. Krueger, 1962: Satellite pictures of mesoscale eddies. *Mon. Wea. Rev.,* **90,** 457–463.

Hunt, C. R., and W. H. Snyder, 1980: Experiments on stably and neutrally stratified flow over a model three dimensional hill. *J. Fluid Mech.,* **96,** 671–704.

Janjić, Z. I., 1990: The step-mountain coordinate: Physical package. *Mon. Wea. Rev.,* **118,** 1429–1443.

——, 1994: The step-mountain Eta coordinate model: Further developments of the convection, viscous sublayer, and turbulence closure schemes. *Mon. Wea. Rev.,* **122,** 927–945.

Koračin, D., and C. E. Dorman, 2001: Marine atmospheric boundary layer divergence and clouds along California in June 1996. *Mon. Wea. Rev.,* **129,** 2040–2056.

Kundu, P. K., 1990: *Fluid Mechanics.* Academic Press, 638 pp.

Kuo, Y.-H., L. Cheng, and J.-W. Bao, 1988: Numerical simulation of the 1981 Sichuan flood. Part I: Evolution of a mesoscale southwest vortex. *Mon. Wea. Rev.,* **116,** 2481–2504.

McKendry, I. G., and C. G. Revell, 1992: Mesoscale eddy development over south Auckland—A case study. *Wea. Forecasting,* **7,** 134–142.

Mellor, G. L., and T. Yamada, 1982: Development of a turbulence closure model for geophysical fluid problems. *Rev. Geophys. Space Phys.,* **20,** 851–875.

Pan, H. L., and L. Mahrt, 1987: Interaction between soil hydrology and boundary-layer development. *Bound.-Layer Meteor.,* **38,** 185–202.

Pedlosky, J., 1987: *Geophysical Fluid Dynamics.* Springer-Verlag, 710 pp.

Pielke, R. A., and M. Segal, 1986: Mesoscale circulations forced by differential terrain heating. *Mesoscale Meteorology and Forecasting,* P. S. Ray, Ed., Amer. Meteor. Soc., 516–548.

Rotunno, R. V., and P. K. Smolarkiewicz, 1991: Further results on lee vortices in low-Froude-number flow. *J. Atmos. Sci.,* **48,** 2204–2211.

——, V. Grubišić, and P. K. Smolakiewicz, 1999: Vorticity and potential vorticity in mountains wakes. *J. Atmos. Sci.,* **56,** 2796–2810.

Schär, C., and R. B. Smith, 1993a: Shallow-water flow past isolated topography. Part I: Vorticity production and wake formation. *J. Atmos. Sci.,* **50,** 1373–1400.

——, and ——, 1993b: Shallow-water flow past isolated topography. Part II: Transition to vortex shedding. *J. Atmos. Sci.,* **50,** 1401–1412.

——, and D. R. Durran, 1997: Vortex formation and vortex shedding in continuously stratified flow past isolated topography. *J. Atmos. Sci.,* **54,** 534–554.

Skamarock, W. C., R. Rotunno, and J. B. Klemp, 2002: Catalina eddies and coastally trapped disturbances. *J. Atmos. Sci.,* **59,** 2270–2278.

Smolarkiewicz, P. K., and R. Rotunno, 1989a: Low Froude number flow past three-dimensional obstacles. Part I: Baroclinically generated lee vortices. *J. Atmos. Sci.,* **46,** 1154–1164.

——, and ——, 1989b: Reply. *J. Atmos. Sci.,* **46,** 3614–3617.

——, R. M. Rasmussen, and T. L. Clark, 1988: On the dynamics of Hawaiian cloud bands: Island forcing. *J. Atmos. Sci.,* **45,** 1872–1905.

Snyder, W. H., R. S. Thompson, and R. E. Eskridge, 1985: The

nature of strongly stratified flow over hills: Dividing streamline concept. *J. Fluid Mech.,* **152,** 249–288.

Stephens, G. L., 1978: Radiation profiles in extended water clouds. II: Parameterization schemes. *J. Atmos. Sci.,* **35,** 2123–2132.

Sun, W.-Y., and J.-D. Chern, 1993: Diurnal variation of lee vortices in Taiwan and the surrounding area. *J. Atmos. Sci.,* **50,** 3404–3430.

——, and ——, 1994: Numerical experiments of vortices in the wakes of large idealized mountains. *J. Atmos. Sci.,* **51,** 191–209.

Vosper, S. B., 2000: Three-dimensional numerical simulations of strongly stratified flow past conical orography. *J. Atmos. Sci.,* **57,** 3716–3739.

Wilczak, J. M., and J. W. Glendening, 1988: Observations and mixed-layer modeling of a terrain-induced mesoscale gyre: The Denver Cyclone. *Mon. Wea. Rev.,* **116,** 1599–1622.

——, W. F. Dabberdt, and R. A. Kropfli, 1991: Observations and numerical-model simulations of the atmospheric boundary layer in the Santa Barbara coastal region. *J. Appl. Meteor.,* **30,** 652–673.